International Journal of Bifurcation and Chaos, Vol. 3, No. 3 (1993) 551–557

BISPECTRAL AND TRISPECTRAL CHARACTERIZATION OF TRANSITION TO CHAOS IN THE DUFFING OSCILLATOR

VINOD CHANDRAN* and STEVE ELGAR
School of Electrical Engineering and Computer Science,
Washington State University, Pullman, WA 99164-2752, USA

CHARLES PEZESHKI
Department of Mechanical and Materials Engineering,
Washington State University, Pullman, WA 99164-2752, USA

Received August 13, 1992; Revised November 19, 1992

Higher-order spectral (bispectral and trispectral) analyses of numerical solutions of the Duffing equation with a cubic stiffness are used to isolate the coupling between the triads and quartets, respectively, of nonlinearly interacting Fourier components of the system. The Duffing oscillator follows a period-doubling intermittency catastrophic route to chaos. For period-doubled limit cycles, higher-order spectra indicate that both quadratic and cubic nonlinear interactions are important to the dynamics. However, when the Duffing oscillator becomes chaotic, global behavior of the cubic nonlinearity becomes dominant and quadratic nonlinear interactions are weak, while cubic interactions remain strong. As the nonlinearity of the system is increased, the number of excited Fourier components increases, eventually leading to broad-band power spectra for chaos. The corresponding higher-order spectra indicate that although some individual nonlinear interactions weaken as nonlinearity increases, the number of nonlinearly interacting Fourier modes increases. Trispectra indicate that the cubic interactions gradually evolve from encompassing a few quartets of Fourier components for period-1 motion to encompassing many quartets for chaos. For chaos, all the components within the energetic part of the power spectrum are cubically (but not quadratically) coupled to each other.

1. Introduction

Higher-order spectra provide information about energy exchange between, and phase coupling among, the modes of motion (i.e., the Fourier components) of nonlinear systems. Since its introduction [Hasselman, 1963], bispectral analysis has been used to investigate quadratic nonlinear interactions in fluid [Yeh & Van Atta, 1973; Lii *et al.*, 1976; Helland *et al.*, 1977; Van Atta, 1979; Kim *et al.*, 1980; Miksad *et al.*, 1983; Ritz *et al.*, 1988], mechanical [Sato *et al.*, 1977; Choi *et al.*, 1984; Pezeshki *et al.*, 1990], and quantum mechanical [Miller, 1986] systems (see Nikias & Raghuveer [1987] for a review). Period-doubling and other quadratic phenomena in the dynamics of the Duffing oscillator were investigated using bispectral techniques [Pezeshki *et al.*, 1990]. However, since the dominant nonlinearity of the Duffing system is cubic, the bispectrum only partially characterizes the system and trispectral techniques [Dalle Molle & Hinich, 1989; Lutes & Chen, 1991] are required for a fuller understanding of the dynamics. In particular, when the system

*Vinod Chandran is currently with the Electrical and Electronic Systems Engineering Department, Queensland University of Technology, Brisbane, Queensland 4001, Australia.

is chaotic the bicoherence spectrum is statistically indistinguishable from that for Gaussian random noise [Pezeshki *et al.*, 1990]. In the present study, trispectral analysis is used to demonstrate that cubic nonlinear interactions occur as the Duffing system undergoes a period-doubling route to chaos. For limit cycles, tricoherence spectra isolate the individual cubic interactions between quartets of Fourier components, especially those associated with oscillations at the power spectral primary peak frequency and its sub- and super-harmonics, as well as their combinations tones. Once the system enters chaos the power spectrum broadens, but the tricoherence spectra still isolate individual nonlinearly coupled quartets. Moreover, the tricoherences suggest that during chaos all the energetic motions are involved in cubic nonlinear interactions, and are coupled to each other.

The paper is organized as follows. Relevant higher-order spectral quantities and the details of the numerical processing are presented in Sec. 2. Bicoherence and tricoherence spectra of the Duffing oscillator are presented in Sec. 3 along with discussions of mode coupling as the system period-doubles and becomes chaotic. Conclusions follow in Sec. 4.

2. Higher-Order Spectra and Numerical Details

A discretely sampled time series $x(t)$ has a Fourier representation given by

$$x(t) = \sum_n [X(\omega_n)\mathrm{e}^{j\omega_n t} + X^*(\omega_n)\mathrm{e}^{-j\omega_n t}], \quad (1)$$

where t is time, X is the complex Fourier coefficient at radian frequency ω_n, and the subscript n is a frequency (modal) index. The power spectrum $P(\omega_1)$, the (auto) bispectrum $B(\omega_1, \omega_2)$, and the (auto) trispectrum $T(\omega_1, \omega_2, \omega_3)$ are defined, respectively, as

$$P(\omega_1) = E[X(\omega_1)X^*(\omega_1)], \quad (2)$$

$$B(\omega_1, \omega_2) = E[X(\omega_1)X(\omega_2)X^*(\omega_1 + \omega_2)], \quad (3)$$

$$T(\omega_1, \omega_2, \omega_3) = E[X(\omega_1)X(\omega_2)X(\omega_3)X^*(\omega_1 + \omega_2 + \omega_3)] \quad (4)$$

where an asterisk denotes complex conjugate, and $E[\ ]$ is the expectation operator. In practice, the expectation operation is replaced by an ensemble average to yield estimates of the respective spectra. The normalized magnitude of the bispectrum, known as the squared *bicoherence*, is given by

$$b^2(\omega_1, \omega_2) = \frac{|B(\omega_1, \omega_2)|^2}{P(\omega_1)P(\omega_2)P(\omega_1 + \omega_2)}. \quad (5)$$

It is well-known [Kim & Powers, 1979] that the bicoherence represents the fraction of power at the triad of frequencies that is owing to quadratic interactions. Similarly, the normalized magnitude of the trispectrum, referred to as the squared *tricoherence*, is given by

$$t^2(\omega_1, \omega_2, \omega_3) = \frac{|T(\omega_1, \omega_2, \omega_3)|^2}{P(\omega_1)P(\omega_2)P(\omega_3)P(\omega_1+\omega_2+\omega_3)}, \quad (6)$$

and the squared tricoherence represents the fraction of power at the quartet of frequencies that is owing to cubic interactions. For a time series with Nyquist frequency ω_N (that is, the highest frequency component for which the spectrum of the time series is nonzero or non-negligible), the bicoherence is unique within a triangle with vertices at $(\omega_1 = 0, \omega_2 = 0)$, $(\omega_1 = \omega_N/2, \omega_2 = \omega_N/2)$, and $(\omega_1 = \omega_N, \omega_2 = 0)$. It is also completely described by values in this triangle if there is no bispectral aliasing. The tricoherence is uniquely defined within a pyramid in trifrequency space, whose base is the triangle referred to above (lying on the plane $\omega_3 = 0$) and whose apex is $(\omega_1 = \omega_N/3, \omega_2 = \omega_N/3, \omega_3 = \omega_N/3)$. Although this is not the complete nonredundant region of computation of the tricoherence [Chandran & Elgar, 1993], it is sufficient here.

The time series analyzed were generated by numerically integrating the Duffing equation using a classic fourth order Runge–Kutta subroutine with an integrating time step of 0.0625 sec for a system with a fundamental period of 6.28 secs. A 1000 sec interval was discarded to allow the transient response to decay after starting from zero initial conditions. The remaining 16384 sec long time series were sampled at 2.0 Hz for power spectral, bispectral, and trispectral analyses. Thus, each time series consisted of 32768 samples and was divided into 256 blocks. Each 64 sec long block was Fourier transformed to yield the complex Fourier coefficients $X(\omega_n)$ with a frequency resolution of 0.015625 Hz. A Hanning window was used on each block to reduce leakage. Power spectra, bispectra, and trispectra were calculated from each 64 sec block and then

averaged over the ensemble of 256 blocks, producing estimates with 512 degrees of freedom. It is well-known that for Gaussian noise the true values of the bicoherence and tricoherence are zero [Hasselmann, 1963; Nikias & Raghuveer, 1987; Dalle Molle & Hinich, 1989]. The 99% significance level for estimates of bicoherence and tricoherence for Gaussian noise are given by $\sqrt{9.2/\mathrm{dof}}$, where dof is the number of degrees of freedom of the estimate [Elgar & Guza, 1988; Chandran *et al.*, 1993]. Thus, bicoherence and tricoherence values above 0.134 are significant at the 99% significance level for 512 degrees of freedom. The addition of noise to the time series results in a decrease in higher-order spectral values such that the bicoherence and tricoherence still represent the fraction of phase coupled power, which is proportionally reduced owing to the presence of uncoupled noise.

3. Results

In this section, phase portraits, power spectra, bicoherence spectra, and tricoherence spectra for the Duffing oscillator as it undergoes a period-doubling route to chaos are presented.

3.1. *The Duffing oscillator*

The model for the Duffing oscillator used here is [Dowell & Pezeshki, 1986]

$$\ddot{u} + \gamma\dot{u} - 0.5(u - u^3) = F\cos(\omega t)\,, \qquad (7)$$

where u is the displacement, $\gamma = 0.168$, $\omega = 1$, F is the amplitude of the forcing, and the overdot denotes differentiation with respect to time t. This equation, which is a second order differential equation with a cubic nonlinear term, in addition to linear damping and stiffness terms, is commonly referred to as a Duffing equation with a negative linear stiffness. The Duffing system has a range of nonlinear behavior [Dowell & Pezeshki, 1988], including periodic and chaotic motions as F is varied.

There exists a strong set of modal couplings in the oscillator output because of the nonlinearity, resulting in energy exchange between, and phase coupling among, the modes of oscillation. These nonlinear interactions cannot be detected by the power spectrum because it does not contain any phase information. On the other hand, bispectral analysis isolates the quadratic phase coupling between triads of oscillations. Although the bicoherence is significant for periodic motions [Pezeshki *et al.*, 1990], it fails to characterize chaotic motion in the Duffing oscillator because the dominant nonlinearity in the system is cubic. Consequently, trispectral analysis is used here to isolate the cubic nonlinear interactions between quartets of Fourier modes as the Duffing system undergoes a period-doubling route to chaos.

3.2. *Phase portraits and power spectra*

Phase portraits of the limit cycles of the Duffing equation as it undergoes a period-doubling sequence to chaos are shown in Fig. 1. Figure 1(a–c) shows period-1, period-2, and period-4 motion respectively. This cascade ends with a saddle-node bifurcation catastrophe with intermittency [Lichtenberg & Liebermann, 1983; Thompson & Stewart, 1986] leading to the attractor shown in Fig. 1(d). The corresponding power spectra are shown in Fig. 2. The period-1 spectrum [Fig. 2(a)] consists

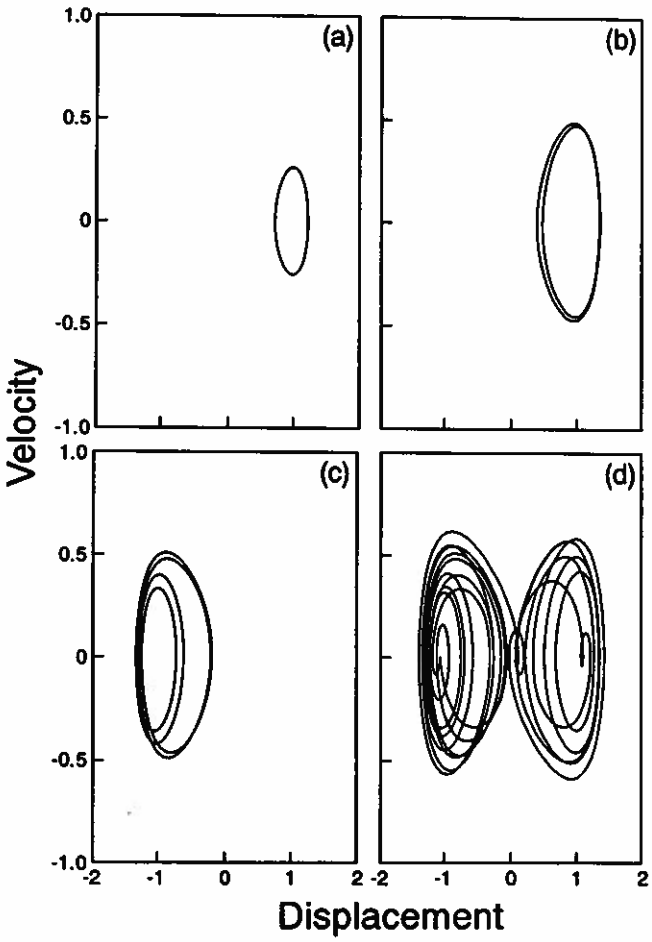

Fig. 1. Phase portraits for the Duffing oscillator, velocity ($\dot{u}$) *vs* displacement (u). (a) period-1 motion, $F = 0.05$; (b) period-2 motion, $F = 0.178$; (c) period-4 motion, $F = 0.197$; (d) chaotic motion, $F = 0.210$.

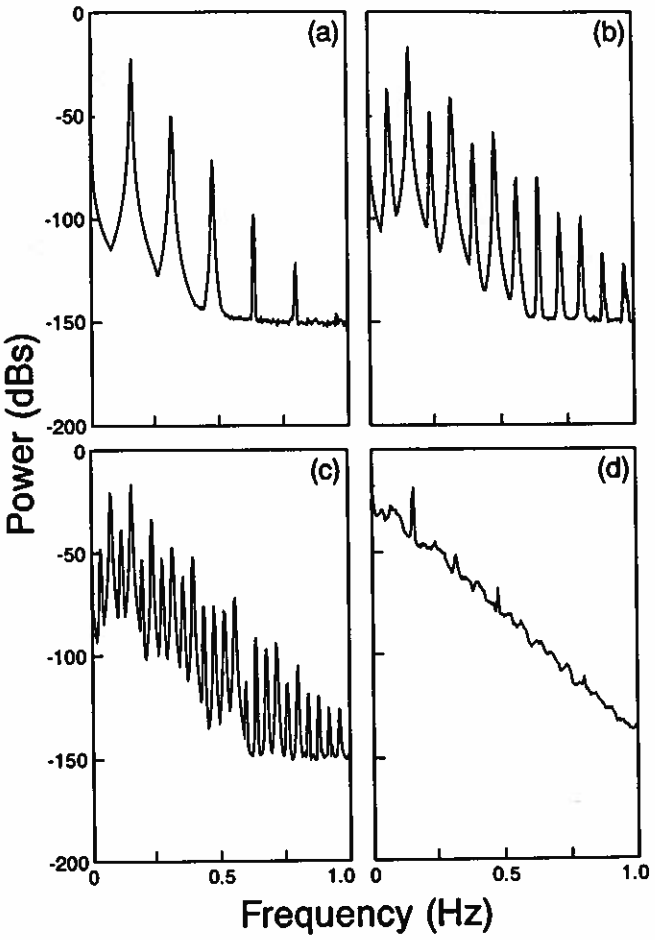

Fig. 2. Power spectra for the Duffing oscillator. (a) period-1 motion; (b) period-2 motion; (c) period-4 motion; (d) chaotic motion. The units of power are arbitrary.

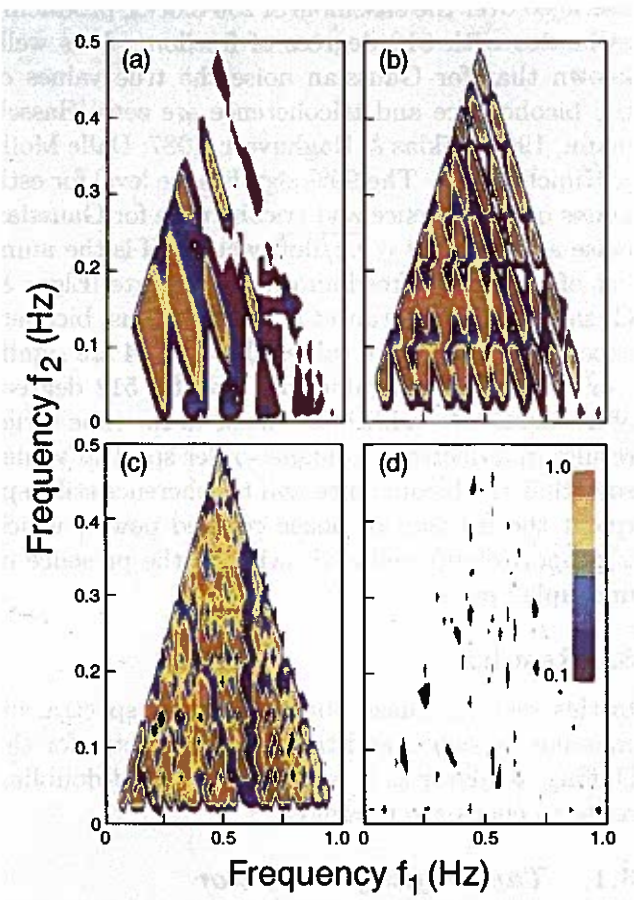

Fig. 3. Contours of bicoherence for the Duffing oscillator. (a) period-1 motion; (b) period-2 motion; (c) period-4 motion; (d) chaotic motion. The minimum contour is $b = 0.1$ with contours every 0.1125 up to $b = 1.0$. The regions between the contours are colored as shown by the scale in (d). The three modes of each triad are f_1, f_2 and $f_1 + f_2$.

of a primary peak at $f = 0.16$ Hz [the driving frequency in Eq. (7)] and its superharmonics. The period-2 spectrum [Fig. 2(b)] has a subharmonic peak at $f = 0.08$ Hz, one half of the driving frequency and a new set of superharmonics corresponding to harmonics and combinations of the two lower-frequency spectral peaks. The period-4 spectrum [Fig. 2(c)] has an additional subharmonic at $f = 0.04$ Hz and additional combination tones. When the system becomes chaotic [Fig. 2(d)], the power spectrum becomes quite broadband with significantly increased energy levels at low frequencies.

3.3. *Bicoherence spectra*

The bicoherence spectra for the four cases are shown in Fig. 3. For period-1 motion [Fig. 3(a)], the bicoherence is high at bifrequencies involving the driving frequency ($f_2 = 0.16$ Hz) and its superharmonics ($f_1 = 0.16$, 0.32, 0.48 Hz, etc). The spreading of bispectral values around the peaks is owing to leakage [Chandran & Elgar, 1991]. As the force amplitude F is increased, resulting in period-doubling, additional clusters of high bicoherence are generated corresponding to the additional modes of motion that are excited [Fig. 3(b)]. The period-quadrupled limit cycle [Fig. 3(c)] indicates a merging of the bicoherence peaks and a weakening of many of the individual bicoherences (i.e., weakening of the individual quadratic nonlinear interactions) as additional frequencies are generated by period-doubling. Finally, when the system becomes chaotic [Fig. 3(d)] quadratic interactions have weakened to an extent that there are hardly any bicoherence values above the 99% significance level. The bicoherence spectrum for the chaotic system is thus indistinguishable from that for a Gaussian random noise process [Pezeshki *et al.*, 1990].

3.4. *Tricoherence spectra*

Tricoherence spectra for the four cases are shown as slices in trifrequency space along the plane $f_3 = 0.16$ Hz (the driving frequency) in Fig. 4. Note that the tricoherence at the quartet consisting of $f_1 = 0.16$, $f_2 = 0.16$, $f_3 = 0.16$, and $f_4 = 0.48$ Hz continues to be significant as the system period doubles [Fig. 4(a–c)] and even when it becomes chaotic [Fig. 4(d)]. The tricoherence spectra for period-1, period-2, and period-4 motions, shown in Figs. 4(a), 4(b), and 4(c) respectively, are similar to the corresponding bicoherence spectra, indicating that the additional frequencies generated by period-doubling are also cubically phase-coupled to the driving frequency. The tricoherence spectrum for chaotic motion [Fig. 4(d)] shows that the tricoherence is significant over a large region in trifrequency space indicating that cubic interactions are important when the system is in chaos. The tricoherence spectrum, therefore, characterizes this chaotic motion as being associated with a cubic nonlinearity. The phase coupling of the first subharmonic ($f_3 = 0.08$ Hz) of the driving frequency with other frequencies is shown in Fig. 5. Similarly, the phase coupling between the mode with frequency 0.24 Hz and other modes is shown in Fig. 6. As shown in Figs. 4–6, the tricoherence is significant for quartets consisting of the primary mode of motion and its sub- and super-harmonics both for period-doubled

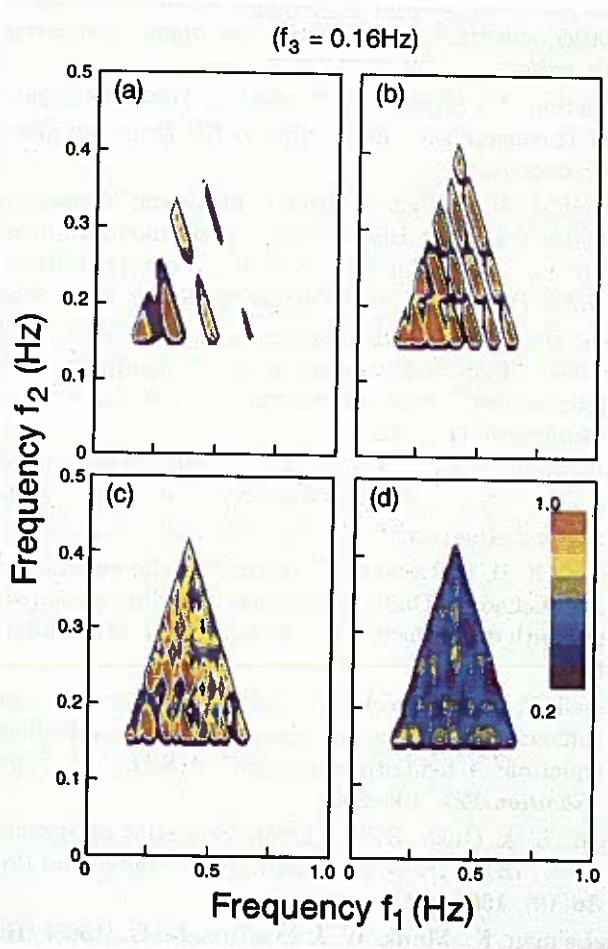

Fig. 4. Contours of tricoherence for the Duffing oscillator when $f_3 = 0.16$ Hz as a function of the other two frequencies, f_1 and f_2: (a) period-1 motion; (b) period-2 motion; (c) period-4 motion; (d) chaotic motion. The minimum contour is $t = 0.2$ with contours for every 0.1 up to $t = 1.0$. The regions between the contours are colored as shown by the scale in (d). The four modes of each quartet are f_1, f_2, $f_3 = 0.16$, and $f_1 + f_2 + f_3$.

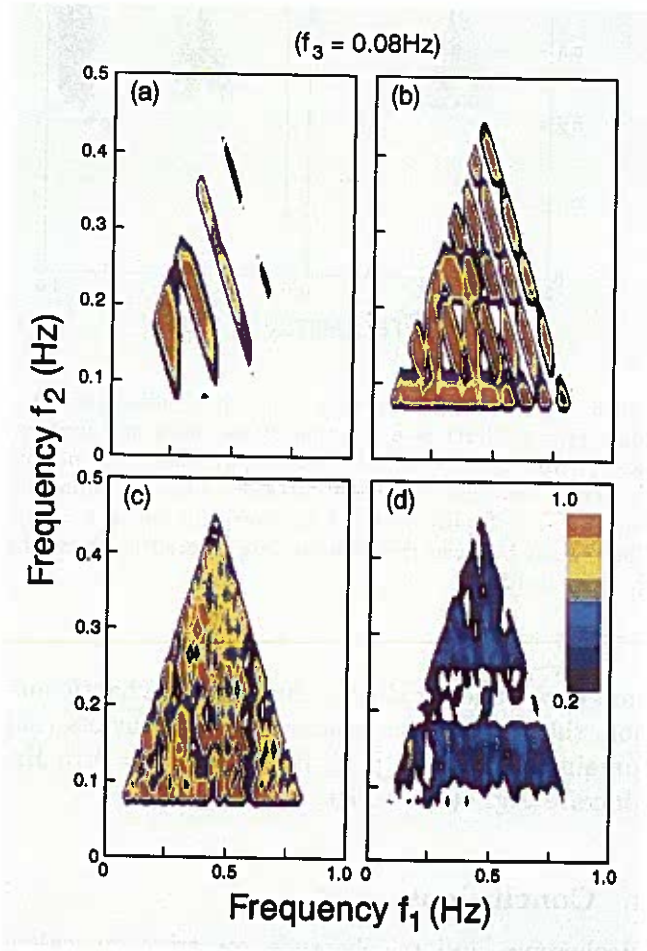

Fig. 5. Contours of tricoherence for the Duffing oscillator when $f_3 = 0.08$ Hz as a function of the other two frequencies, f_1 and f_2: (a) period-1 motion; (b) period-2 motion; (c) period-4 motion; (d) chaotic motion. The minimum contour is $t = 0.2$ with contours for every 0.1 up to $t = 1.0$. The regions between the contours are colored as shown by the scale in (d).

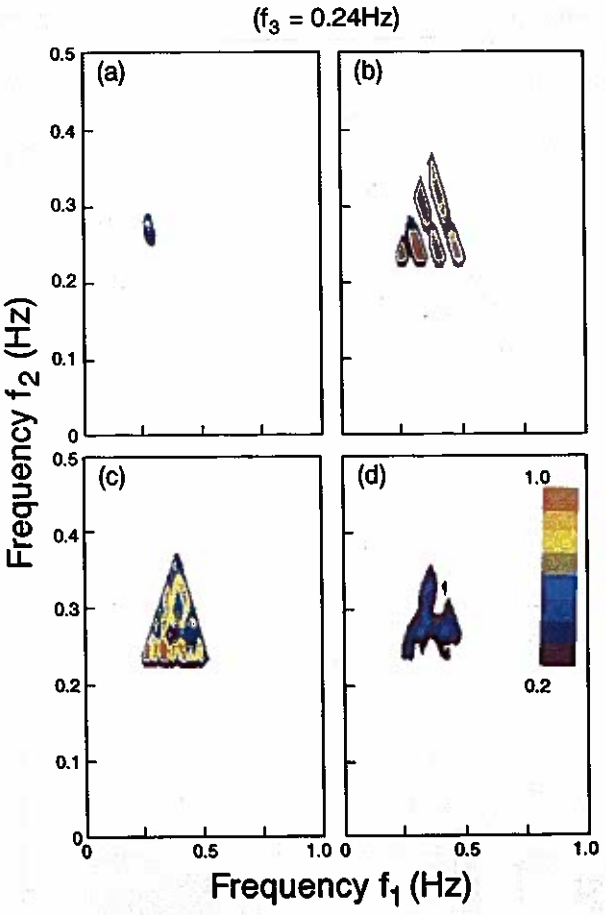

Fig. 6. Contours of tricoherence for the Duffing oscillator when $f_3 = 0.24$ Hz as a function of the other two frequencies, f_1 and f_2: (a) period-1 motion; (b) period-2 motion; (c) period-4 motion; (d) chaotic motion. The minimum contour is $t = 0.2$ with contours for every 0.1 up to $t = 1.0$. The regions between the contours are colored as shown by the scale in (d).

limit cycles and for chaotic motion. For chaotic motion, the tricoherence is strongest for quartets that contain the primary peak frequency [$f = 0.16$ Hz, compare Fig. 4(d) to Figs. 5(d) and 6(d)].

4. Conclusions

Bicoherence and tricoherence spectra were calculated for numerical simulations of a period-doubling cascade of the Duffing oscillator. The periodic trajectories (limit cycles) possessed strong bicoherence and tricoherence originating primarily about the driving frequency, suggesting that quadratic and cubic nonlinear interactions between modes of motion are important to the dynamics of periodic motion. The chaotic trajectory was characterized by statistically insignificant bicoherence, but statistically significant tricoherence, consistent with the cubic nature of the dominant nonlinearity.

Acknowledgments

This research was supported by the Office of Naval Research (Nonlinear Ocean Waves ARI and Coastal Sciences) and the National Science Foundation (Physical Oceanography). Discussions with Mr. Amit Athalye are gratefully acknowledged.

References

Chandran, V. & Elgar, S. [1993] "A general procedure for the computation of principal domains of higher-order spectra," *IEEE Trans. on Signal Processing, in press.*

Chandran, V., Elgar, S. & Vanhoff, B. [1993] "Statistics of Tricoherence," submitted to *IEEE Trans. on Signal Processing.*

Chandran, V. & Elgar, S. [1991] "Mean and Variance of Estimates of the Bispectrum of a Harmonic Random Process — An Analysis Including Leakage Effects," *IEEE Trans. on Signal Processing* **39**(12), 2640–2651.

Choi, D., Chang, J. H., Stearman, R. & Powers, E. J. [1984] "Bispectral identification of nonlinear mode interactions," *Proc. of the 2nd Intl. Modal Analysis Conference* **II**, 3–12.

Dalle Molle, J. W. & Hinich, M. J. [1989] "The Trispectrum," *Proc. of the Workshop on Higher-Order Spectral Analysis* 68–72, Vail, Colorado, June 28–30.

Dowell, E. H. & Pezeshki, C. [1986] "On the understanding of chaos in Duffings equation including a comparison with experiment," *A.S.M.E. J. Appl. Mech.* **53**(1), 5–9.

Dowell, E. H. & Pezeshki, C. [1988] "On necessary and sufficient conditions for chaos to occur in Duffings equation: A heuristic approach," *A.S.M.E. J. Sound Vibration* **121**, 195–200.

Elgar, S. & Guza, R. T. [1988] "Statistics of Bicoherence," *IEEE Trans. on Acoust. Speech and Signal Proc.* **36**(10), 1667–1668.

Hasselman, K., Munk, W. & MacDonald, G. [1963] "Bispectra of Ocean Waves," *Time Series Analysis*, ed. Rosenblatt, M. (John Wiley, New York) pp. 125–139.

Helland, K. N., Van Atta, C. W. & Stegun, G. N. [1977] "Spectral energy transfer in high Reynolds number turbulence," *J. Fluid Mech.* **79**, 337–359.

Kim, Y. C. & Powers, E. J. [1979] "Digital bispectral analysis and its applications to nonlinear wave interactions," *IEEE Trans. Plasma Science* **PS-7**, 120–131.

Kim, Y. C., Beall, J. M., Powers, E. J. & Miksad, R. W. [1980] "Bispectrum and nonlinear wave coupling," *Phys. Fluids* **21**(8), 258–263.

Lichtenberg, A. J. & Lieberman, M. A. [1983] *Regular and Stochastic Motion* (Springer Verlag, New York).

Lii, K. S., Rosenblatt, M. & Van Atta, C. [1976] "Bispectral Measurements in Turbulence," *J. Fluid Mech.* **77**, 45–62.

Lutes, L. D. & Chen, D. C. K. [1991] "Trispectrum for the response of a non-linear oscillator," *Internat. J. Non-Linear Mech.* **26**(6), 893–909.

Miksad, R., Jones, F. & Powers, E. J. [1983] "Measurements of nonlinear interactions during natural transitions of a symmetric wake," *Phys. Fluids* **26**, 1402–1409.

Miller, M. [1986] "Bispectral analysis of the driven Sine-Gordon chain," *Phys. Rev.* **B34**, 6326–6333.

Nikias, C. L. & Raghuveer, M. R. [1987] "Bispectrum estimation: A digital signal processing framework," *IEEE Proceedings* **75**(7), 869–891.

Pezeshki, C., Elgar, S. & Krishna, R. C. [1990] "Bispectral analysis of systems possessing chaotic motion," *J. Sound Vibration* **137**(3), 357–368.

Ritz, C., Powers, E. J., Miksad, R. & Solis, R. [1988] "Nonlinear spectral dynamics of a transitioning flow," *Phys. Fluids* **31**, 3577–3588.

Sato, T., Sasaki, K. & Nakamura, Y. [1977] "Real-time bispectral analysis of gear noise and its application to contactless diagnosis," *J. Acoust. Soc. Amer.* **62**(2), 382–387.

Thompson, J. B. & Stewart, H. B. [1986] *Nonlinear Dynamics and Chaos* (John Wiley, New York).

Van Atta, C.W. [1979] "Inertial range bispectra in turbulence," *Phys. Fluids* **22**, 1440–1443.

Yeh, T. T. & Van Atta, C. W. [1973] "Spectral transfer of scalar and velocity fields in heated-grid turbulence," *J. Fluid Mech.* **58**, 233–261.

Appendix

The sinusoidal forcing function is the only source of external excitation for the Duffing oscillator, and the nonlinearities present in the system are responsible for redistributing the signal energy to the higher harmonics. It is not very obvious how a system with cubic and linear stiffness terms seems to be dominated by a quadratic nonlinearity for part of its behavior. An explanation can be provided by using a Taylor series expansion of the first-order form of the differential equation about its fixed points. The Duffing system in state space form is

$$\dot{u}_1 = u_2\,, \tag{8}$$

$$\dot{u}_2 = -0.168u_2 + 0.5(u_1 - u_1^3)\,. \tag{9}$$

The Taylor series expansion up to third order is given by

$$\delta\dot{U}_1 = \delta U_2\,, \tag{10}$$

$$\begin{aligned}\delta\dot{U}_2 = &-0.168\delta U_2 + 0.5(1 - 3U_1^2)\delta U_1 \\ &- 3U_1(\delta U_1)^2 - 0.5(\delta U_1)^3\,,\end{aligned} \tag{11}$$

where δU_1 and δU_2 are the perturbation variables about the fixed point, and U_1 and U_2 are the values of the phase variables at the fixed points. When the motion is centered around the stable fixed points $(1,0)$ and $(-1,0)$, as is the case for the period-doubled limit cycles, the quadratic nonlinearity plays a dominant role in the system. It can be observed from the phase portraits that $\delta U_1 < 1$ away from the fixed point for any of the period-doubled limit cycles, so that $(\delta U_1)^3$ will be small. Once the system goes into chaos, trajectories of the system surround all the fixed points. The cubic behavior will then dominate, and this is directly observed by examining the high values in the tricoherence spectrum and the corresponding low values in the bicoherence spectrum.

Coupled sets of nonlinear equations can be feedback loops, and depending on the parameter values and the type of equation, are capable of generating any number of higher harmonics. All these harmonics may then be phase-coupled to the same fundamental mode, yielding high values for several different higher-order coherences. For example, if ω_1 is coupled to ω_2 to yield $\omega_3 = \omega_1 + \omega_2$, and ω_2 is coupled to ω_3 to yield $\omega_4 = \omega_2 + \omega_3$, then the tricoherence at the quartet ω_1, ω_2, $\omega_1 + \omega_2$, $\omega_1 + \omega_2 + \omega_2$ will be high, although the governing mechanism behind energy redistribution is quadratic. The period-doubled limit cycles for the Duffing oscillator exhibit both high bicoherence and high tricoherence at the modal groups of interest, and the energy redistribution for such motion may be attributed to a dominant quadratic nonlinearity and feedback.